Journal of Bio- and Tribo-Corrosion (2023) 9:77
https://doi.org/10.1007/s40735-023-00798-x

How the Behavior of Tribocorrosion of Biocomposites Containing Mollusc Shell Particles is Affected by Potential in the Presence of Bovine Serum Solution?

Besma Sidia[1] · **Walid Bensalah**[1]

Received: 23 March 2023 / Revised: 15 July 2023 / Accepted: 5 September 2023 / Published online: 25 September 2023
© The Author(s), under exclusive licence to Springer Nature Switzerland AG 2023

Abstract

Corrosion of the metal component and polymer wear debris in hip joint prostheses is a major problem for many patients. The aim of this study was two-fold: first, to assess the potential of mollusc shells (MS) as reinforcements for polymers and second, to gain a better understanding of the corrosion phenomenon occurring at composite–metal interfaces in dry and bovine serum solution, which mimics the lubricating and nourishing properties of synovial fluid. To achieve this aim, a tribocorrosion study was carried out using a reciprocating pin-on-disk tribocorrosimeter coupled with a potensiostat galvanostat. MS–HDPE biocomposites, filled with 0, 5, 10, and 15 wt% of MS, were elaborated by hot compressing molding process. The open-circuit potential of the Ti6Al4V pin in contact with the biocomposite was examined and the impact of MS filler on the coefficient of friction and wear behavior was analyzed. The study proposed a damage mode and wear scenario for the MS–HDPE composite when exposed to bovine serum solution. In particular, the effect of bovine serum protein adsorption was analyzed. The results showed that the addition of MS particles affected the corrosion behavior of the Ti6Al4V pin. The results indicated that the optimum MS content was approximately 5 wt% with 50% reduction in the specific wear rate in bovine serum solution. SEM images showed that the morphology of the worn surface of 5-wt% MS–HDPE presents a better surface morphology compared to 10-wt% MS–HDPE. Finally, 5 wt% of MS–HDPE may be an interesting candidate for orthopedic applications.

Keywords Biocomposite · Tribocorrosion · Mollusc shell filler · Bovine serum · Wear resistance

Abbreviations

MS	Mollusc shell
MoP	Metal-on-polymer
MoM	Metal-on-metal
HAP	Hydroxyapatite
HDPE	High-density polyethylene
SEM	Scanning electron microscope
WE	Working electrode
RE	Reference electrode
CE	Counter electrode
SCE	Saturated calomel electrode
OCP	Open-circuit potential

✉ Besma Sidia
sidia.besma@gmail.com

[1] Mechanical Engineering Laboratory, National Engineering School of Monastir, University of Monastir, LR99ES32, Monastir, Tunisia

1 Introduction

Tribocorrosion research has gained momentum and is becoming an active field of study owing to its prevalence in various scientific fields, including automotive, petroleum, and biomedical applications [1, 2]. It merges the disciplines of tribology and corrosion [3] and cannot be predicted solely on the basis of isolated material wear and corrosion behaviors. In fact, the combined effects of these processes can lead to accelerated wear in tribocorrosion tests [4, 5].

The tribocorrosion process has become increasingly important in biomedical applications. Hip joint prostheses experience repetitive loading, friction, and corrosive environments within the body. The tribocorrosion behavior of the components can significantly affect their wear resistance, mechanical stability, and overall performance [5–7]. Two types of material pairs are commonly used in hip implants, namely Metal-on-Polymer (MoP) and Metal-on-Metal (MoM) friction torques [5, 8]. In France, MoP pairs are the most frequently used for hip prosthesis implants, accounting

for 45% of global implantations [9]. This study focused on examining the MoP friction torque. Patients with a MoP hip prosthesis can suffer from a number of implant-related problems and complications, including implant wear and degradation; over time, friction and wear on the articulation surfaces of metal and polymer components can lead to the release of debris from wear particles. This later results in local inflammation, tissue reaction, bone loss (osteolysis), accelerated localized corrosion, and ultimately implant failure [10]. Moreover, aseptic loosening of the implant is mainly caused by polymer wear debris and metallic corrosion in the hip joint prosthesis component [11–13]. In fact, when polymer and metal materials come into contact, electrochemical reactions can occur, generating corrosion products or potentially toxic substances [14]. These reactions can trigger inflammatory reactions and undesirable immune responses in the patient [3]. This highlights the need for a better understanding of the electrochemical behavior of the metallic implant component in an environment that closely resembles the living environment of the implant. Additionally, improving the wear resistance of the polymeric component is crucial for enhancing the longevity of the implant. Previous research has investigated the electrochemical behavior of metal implants in various electrolytes, including physiological Ringer's solution [6], saline solution [15], and bovine serum [2]. The development of new biomaterials with improved tribological properties has been a challenge for many years, with materials such as cuttle bone [16], chitosan [17], sea coral [17], and snail shell [18] being studied. As biomaterial, mollusc shell (MS) represents a promising biomaterial, known for its favorable biocompatibility and ability to facilitate the efficient activation of osteogenic cells in animal models [19].

Buciumeanu et al. [20] recently examined the tribocorrosion behavior of biocomposites made of Ti6Al4V charged with hydroxyapatite (HAP), while Zai et al. [21] aimed to improve the wear resistance of the polymer and corrosion resistance of the metallic parts of the CoCrMo/UHMWPE pair by incorporating multilayer graphene particles into the UHMWPE matrix and depositing a zirconia coating on the CoCrMo alloy. Salem et al. [22] investigated the tribocorrosion behavior of high-density polyethylene reinforced by molybdenum disulfide particles (MoS_2-HDPE) against a stainless-steel pin in diluted bovine serum, with different contents of MoS_2 (2, 4, 6, 10, and 25 wt%) being used. The research results show that the Ti6Al4V–HAP biocomposite has relatively low wear and high corrosion resistance compared to pure Ti6Al4V, while the addition of graphene particles to UHMWPE improves its wear resistance. The OCP measurement indicates that the corrosion resistance of CoCrMo–ZrO_2 is better than that of uncoated CoCrMo. However, a significant increase in the wear rate was observed for 4 wt% of MoS_2-HDPE compared to pure HDPE. The OCP of the stainless-steel pin shifted to more positive potentials due to the generation of a protective passive layer on the pin when immersed in bovine serum solution [22].

To the best of our knowledge, no previous research has been conducted into the tribocorrosion characteristics of biocomposites composed of high-density polyethylene (HDPE) reinforced with mollusc shell (MS) particles when they come into contact with Ti6Al4V in the presence of a bovine serum solution. The main aim of this study was first to investigate the impact of incorporating MS particles as a biofiller in HDPE on the polymer's wear resistance and second to gain a better understanding of the corrosion phenomenon occurring at the composite–metal interfaces in the presence of a bovine serum solution. For that, studying the tribocorrosion of composites in contact with metal in the context of hip prostheses enables us to better understand the interactions between these materials, assess implant durability, prevent undesirable effects, and optimize prosthesis performance to ensure a better quality of life for patients.

This study investigates the tribocorrosion behavior of MS–HDPE biocomposites in dry and bovine serum conditions against Ti6Al4V pins. The biocomposites are made by incorporating varying amounts of MS into the HDPE matrix (0, 5, 10, and 15 wt%). The free potential of Ti6Al4V is analyzed electrochemically during the tribocorrosion tests. Additionally, the effect of MS particles on the coefficient of friction and the specific wear rate under both dry and bovine serum conditions is investigated. After wear tests, the wear surface morphology of different biocomposites is examined to determine the optimal MS content. Finally, damage mode and wear scenario of the biocomposite during tribocorrosion testing in the presence of bovine serum is proposed.

2 Materials and Methods

In this study, tribocorrosion behavior of unfilled HDPE and MS–HDPE biocomposite discs was evaluated against Ti6Al4V pin, in the presence of serum bovine solution. Figure 1a presents the cylindrical shape adopted for the

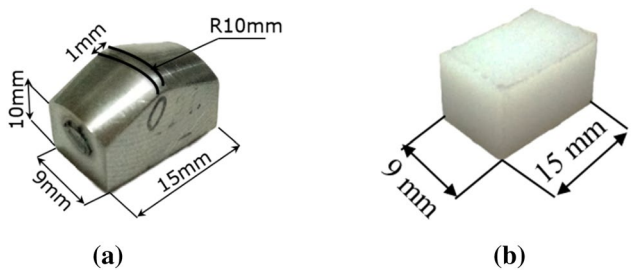

Fig. 1 **a** Ti6Al4V and **b** MS–HDPE biocomposite

Ti6Al4V pins and the chemical composition of Ti6Al4V is given in Table 1.

MS–HDPE biocomposite was prepared with different weight percentage (0, 5, 10, and 15 wt% of MS added to HDPE). The biocomposites are prepared by hot compression molding process as described in our previous work [23]. The obtained composite was, then, machined into target shape as shown in Fig. 1b, giving a linear contact between the metal and the composite.

2.1 Morphological Characteristics

After tribocorrosion tests, wear tracks on the biocomposite disks were investigated using both 3D optical profilometers and scanning electron microscope (SEM). Bruker nasoscope TM, VEECO WyKo NT9100 3D optical profilometer was employed to determine the topographic relief of the wear tracks. This 3D profilometer was coupled with an image processing Viso version 4.20-2002-Scanning Interferometry software. The wear volume (V) was measured using the Bruker nasoscope TM, VEECO WyKo NT9100 3D optical profilometer, analyzing the wear profiles. Using Archard's wear law [Eq. (1)], the specific wear rate (k) was estimated. Equation (1) takes into account the normal load [F_N (N)], total sliding distance [L (m)], and average volumetric wear [ΔV (mm^3)] [24, 25].

$$K = \frac{\Delta V}{F_N.L}. \quad (1)$$

ZEISS Supra 55 VP SEM was equally used to examine the wear tracks of the biocomposite.

2.2 Tribocorrosimeter

Tribocorrosion tests were carried out using a tribocorrosimeter (Fig. 2). This device is animated by a reciprocating linear sliding movement. For an imposed micro-displacement of ± 400 µm and for 15,000 cycles of sliding, a total slip regime was achieved. During the test, a frequency of 1 Hz corresponding to the gait cycle was adopted [26]. The tribocorrosion tests were carried out under normal force of 85 N which is equivalent to 60 MPa of linear contact pressure between the biocomposite disk and the Ti6Al4V pin [23]. The biocomposite sample was immerged in 1:2 aqueous solution of bovine serum as lubricant. The used bovine serum is provided by PAA Laboratory GmbH, (Australia) with 30-g/L protein concentration. Therefore, the biocomposite disk was made to slide against Ti6Al4V pin. During

Table 1 Chemical composition of Ti6Al4V pin

Ti6Al4V								
Element	Al	V	Fe	C	N	H	O	Ti
Composition (wt%)	6.1	4.1	0.15	0.02	0.02	0.006	0.12	Rest

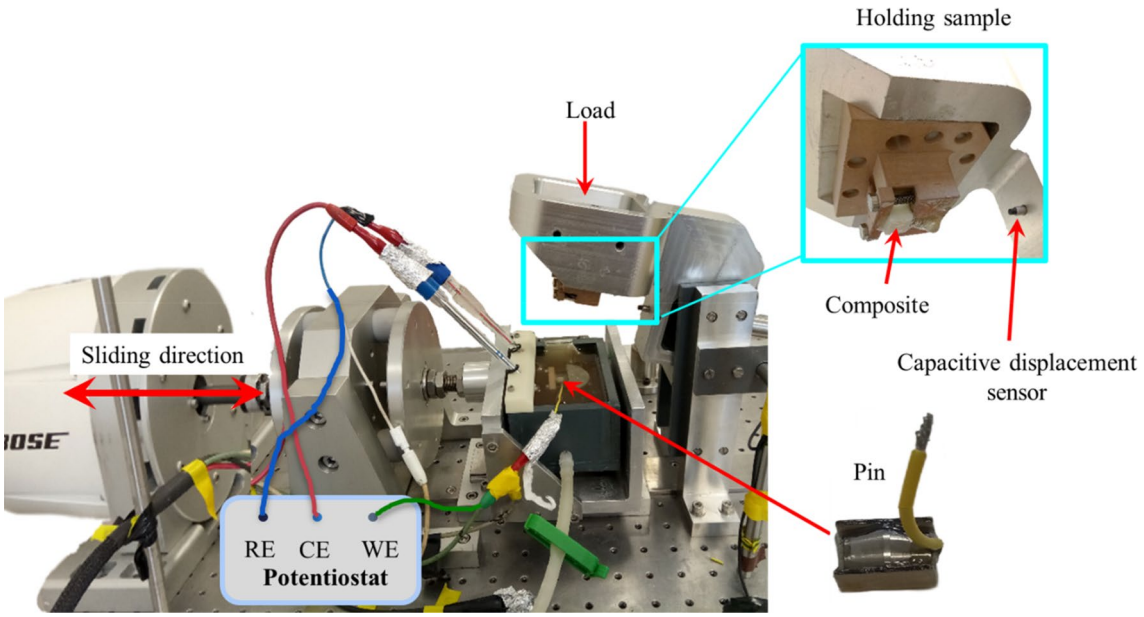

Fig. 2 Tribocorrosimeter

tests, this pin was electrically isolated. For that, zircaloy platelets with undergone heat treatments are glued on the three faces of the Ti6Al4V pin. Additionally, the pin is varnished by specific varnish to ensure good isolation. The tribocorrosimeter is coupled to a load cell. The load cell is a piezoelectric transducer, and the displacement meter is a capacitive sensor. The record of the mechanical data was acquired via Wintest™ and TA Instruments™ software, enabling the coefficient of friction to be calculated.

PARSTAT 2263 potensiostat galvanostat was used to conduct electrochemical measurement. Three electrodes were connected to the potensiostat, namely

- Ti6Al4V pin as working electrode (WE): a copper wire is soldered by point to the pin and then connected to the potensiostat;
- A saturated calomel electrode (SCE, $E = +246$ mV (SHE) at $T = 22°C$) as reference electrode (RE);
- A platinum plate electrode as counter electrode (CE).

Electrochemical measurements were carried out according to four steps (Table 2):

Table 2 Electrochemical measurement steps

Electrochemical steps	
Step 1	Cathodic polarization: − 1 V/SCE during 5 min
Step 2	OCP after polarization during 1 h
Step 3	OCP during 4 h of sliding
Step 4	OCP after sliding during 2 h

3 Results and Discussion

3.1 Open-Circuit Potential (OCP)

Figure 3 shows the evolution of open-circuit potential, OCP, as a function of time during a tribocorrosion test where the cylindrical Ti6Al4V pin is in contact with the MS–HDPE biocomposite in the presence of bovine serum solution.

After a cathodic polarization imposed at − 1 V, the OCP was measured before, during, and after friction.

Before friction, OCP increases rapidly toward more positive potentials until reaching quasi-stationary values for the different biocomposites (0, 5, 10, and 15 wt% of MS). This increase in potential is related to the formation of a passive protective film on Ti6Al4V pin. This result correlates with previous study [27]. This layer is essentially formed by an oxide film and organic molecules of bovine serum adsorbed on the surface of the pin [20, 28, 29].

During 15,000 friction cycles, OCP of the different tribological pairs shows a varied pattern (Fig. 3). For unfilled HDPE, Fig. 3 shows that a slight drop in OCP was measured after 3 h of rubbing. A similar observation has been reported in the literature by Royhman et al. [30], where they suggest that this finding may be related to the damage mechanism of HDPE. In addition, Masdek et al. [31] in their study showed that both 316L and Ti6Al4V in contact with a polymer show stable corrosion resistance in the presence of bovine serum albumin.

For 5, 10, and 15 wt% of MS–HDPE (Fig. 3), a sudden drop in OCP toward more negative values is observed from the beginning of the friction. This abrupt decrease in OCP corresponds to the disturbance and/or destruction of the

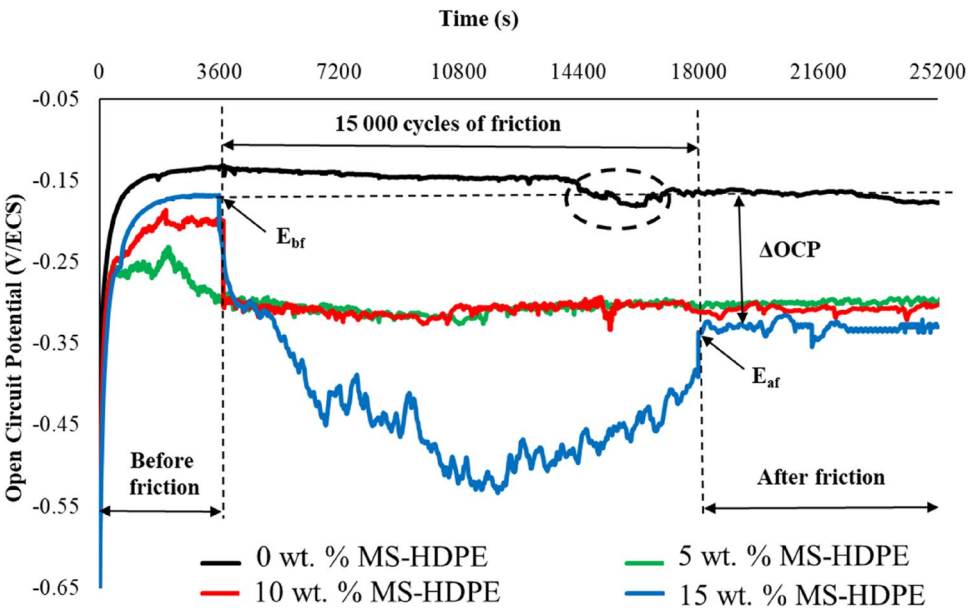

Fig. 3 Evolution of OCP before, during, and after friction of the Ti6Al4V pins against MS–HDPE biocomposites in bovine serum solution

passive layer on the surface of the Ti6Al4V pin, as reported in the literature [27, 32, 33].

After 30 min of friction, the OCP of Ti6Al4V pins rubbing against 5 and 10 wt% of MS–HDPE biocomposites stabilizes. Indeed, the passive layer on the surface of the pins is partially destroyed by friction under the effect of abrasive MS particles at the interface. This constant potential may be due to the alternation created between electrochemical repassivation (construction of the passive film) and mechanical depassivation (damage of the passive film) [34].

On the other hand, with friction, an intense drop in OCP has been recorded for the case of 15 wt% of MS–HDPE biocomposite (Fig. 3). In fact, the protective layer formed on the Ti6Al4V pin was destroyed under reciprocating sliding against the 15-wt% MS–HDPE biocomposite. This phenomenon can be attributed to the presence of more MS debris at the friction interface.

After friction for 15 wt% of MS–HDPE, the OCP has again increased toward more positive values ($E_{endf} \approx$ -0.33 V/ECS) and stabilizes toward values close to those measured against the other biocomposites (5 and 10 wt% of MS–HDPE) (Fig. 3). This increase in OCP toward more noble values reveals the repassivation of the Ti6Al4V pin. The same observations have been mentioned in the literature [15, 32, 33, 35, 36].

3.2 Coefficient of Friction

Figure 4 shows the variation of the coefficient of friction of 0-, 5-, 10-, and 15-wt% MS–HDPE, sliding against Ti6Al4V pins in dry condition, as a function of the number of cycles.

As can be seen in Fig. 4, the coefficients of friction of the different MS–HDPE biocomposites show similar appearances. In fact, from the first number of cycles, the coefficients of friction increase continually until reaching a steady state after 3000 cycles of sliding. In fact, a short running-in period is observed at the initial stage of friction testing. During this period, the asperities of the composite-metal surfaces gradually adapt and wear away, generally resulting in an increase in COF [24]. The friction coefficient of the 0-wt% MS–HDPE biocomposite increased slightly until it reached a value of 0.21 after 15,000 cycles. During friction, HDPE wear debris are generated on the surface of the materials in contact. As the accumulation of debris increases, the COF may also increase, until an equilibrium is reached [24]. It is important to mention that the addition of the MS to HDPE reduces the friction coefficient in dry condition. Indeed, the increase in MS content leads to a greater reduction in the friction coefficient. Moreover, the addition of 5 to 15 wt% of MS–HDPE reduced the friction coefficient by 38, 51, and 75% compared to 0 wt% of MS–HDPE, respectively (Fig. 4). The observed decrease in the frictional behaviors of the biocomposites may be related to the increase in the hardness of the MS–HDPE biocomposite as discussed in our previous work [23].

Figure 5 shows the evolution of the friction coefficient as a function of the number of cycles of the retained biocomposites (0, 5, 10, and 15 wt% of MS–HDPE) rubbing against Ti6Al4V pins in the presence of bovine serum solution.

It can be seen that the different biocomposites show similar patterns in terms of coefficient of friction (Fig. 5). Indeed, at the beginning of the friction, a sudden decrease in the coefficient of friction was observed, followed by an increase and then a tendency toward stabilization.

It is important to mention that, compared to the results obtained under dry condition (Fig. 4), a decrease in the

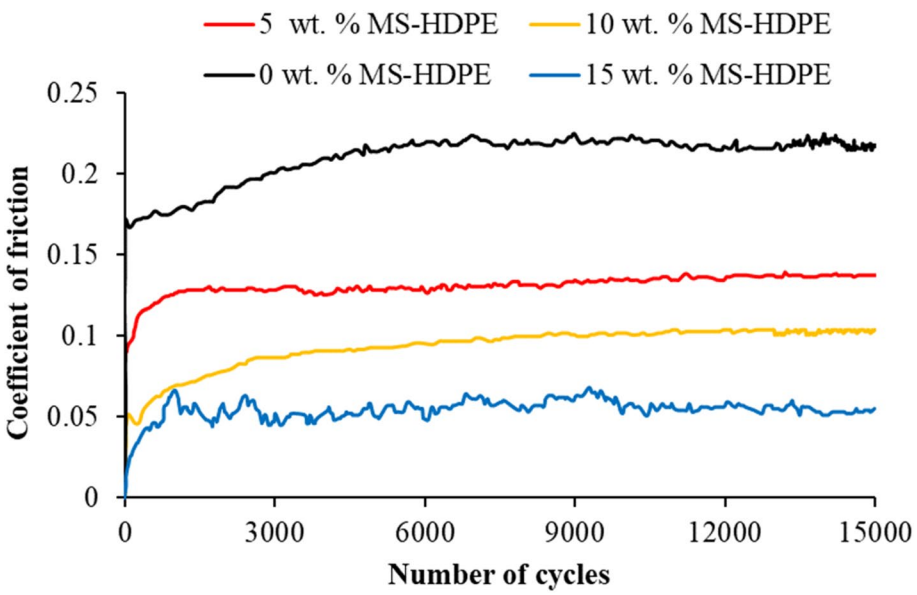

Fig. 4 Evolution of the coefficient of friction of the different biocomposites as a function of the number of cycles in dry condition

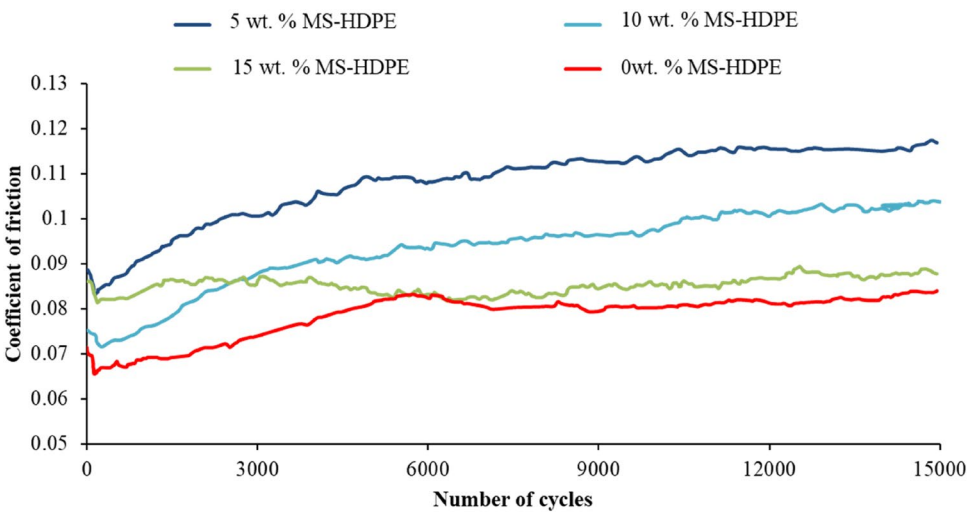

Fig. 5 Evolution of the coefficient of friction of different biocomposites as a function of the number of cycles during tribocorrosion tests

friction coefficient of the biocomposites was observed in the presence of the bovine serum solution (Fig. 5). Indeed, the protein present in the base lubricant of the bovine serum solution has an important effect on the friction behavior of the polymer [37, 38]. For unfilled HDPE (0-wt% MS–HDPE), the coefficient of friction reached a value of 0.083 at the end of the tribocorrosion test, in bovine serum solution. With the addition of 5 wt% of MS, 44% increase in the coefficient of friction was obtained (Fig. 5).

On the other hand, by further increasing the filler rate (10 and 15 wt% of MS–HDPE), the coefficient of friction tends to decrease compared to the 5-wt% MS–HDPE (Fig. 5). These results are consistent with those in the literature [39] and have been linked to the corrosion phenomena of the Ti6Al4V pins in the presence of bovine serum.

In fact, as discussed previously, the addition of MS particles caused the total or partial destruction of the passive protective film on the surface of the pin (Fig. 3). Thereafter, the development of corrosion phenomena causes a progressive roughness of the pin surface, hence the increase in the coefficient of friction [32].

3.3 Wear Behavior

Figure 6 shows the variation of specific wear rate as a function of the different biocomposites (0-, 5-, 10-, and 15-wt% MS–HDPE), after 15,000 cycles of friction against Ti6Al4V pin, in dry condition and in the presence of bovine serum solution.

In dry condition, similar to the friction coefficient, the addition of the MS to HDPE has a positive effect on its

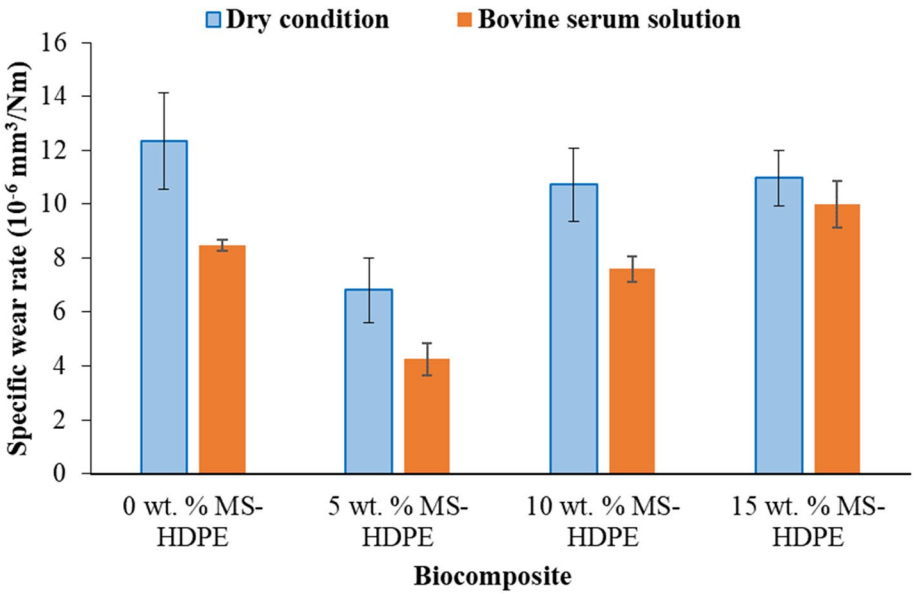

Fig. 6 Variation of the specific wear rate generated on the different MS–HDPE biocomposites after sliding against Ti6Al4V pins, in dry and bovine serum solution

specific wear rate. In fact, the specific wear rate of the 0-wt% MS–HDPE was approximatively around 12.34×10^{-6} mm^3/N m. Moreover, a 44, 13, and 11% reduction in the specific wear rate was obtained with the MS–HDPE biocomposite reinforced by 5, 10, and 15 wt%, respectively (Fig. 6). Similar result was obtained when MS–HDPE biocomposite slides against M30NW pin in our previous study [23]. This improvement in the resistance of the biocomposite is probably related to the increase in its hardness [23].

After tribocorrosion tests in the presence of bovine serum solution, the specific wear rate measured on the wear track of unfilled HDPE is equal to 8.46×10^{-6} mm^3/N mm.

The addition of MS particles shows a significant effect on the wear rate in the presence of bovine serum solution. In fact, for low filler contents (5 wt% of MS–HDPE), a 50% reduction in the specific wear rate compared to the unfilled HDPE was observed (Fig. 6).

However, the addition of more than 5 wt% of MS particles does not have a positive effect on the wear rate. For 10 and 15 wt% of MS, the measured specific wear rates are equal to 7.6×10^{-6} mm^3/N mm and 9.9×10^{-6} mm^3/N mm, respectively (Fig. 6).

It is important to mention that, compared to the results obtained in dry conditions, an improvement in the wear behavior of the biocomposites was observed in the presence of bovine serum solution. In fact, bovine serum albumin interacts with calcium carbonate of the MS particles to form a tribofilm on the biocomposites surface. Consequently, this tribofilm increases the wear resistance of the biocomposite against metallic pin [23, 29].

3.4 Morphological Study

Figure 7 shows three-dimensional topographic relief of the wear marks generated on the different MS–HDPE biocomposites after tribocorrosion tests, in bovine serum solution.

As shown in Fig. 7a, the wear of unfilled HDPE (0 wt% of MS–HDPE) is dominated by plastic deformation of the material. Indeed, parallel grooves in the sliding direction were observed.

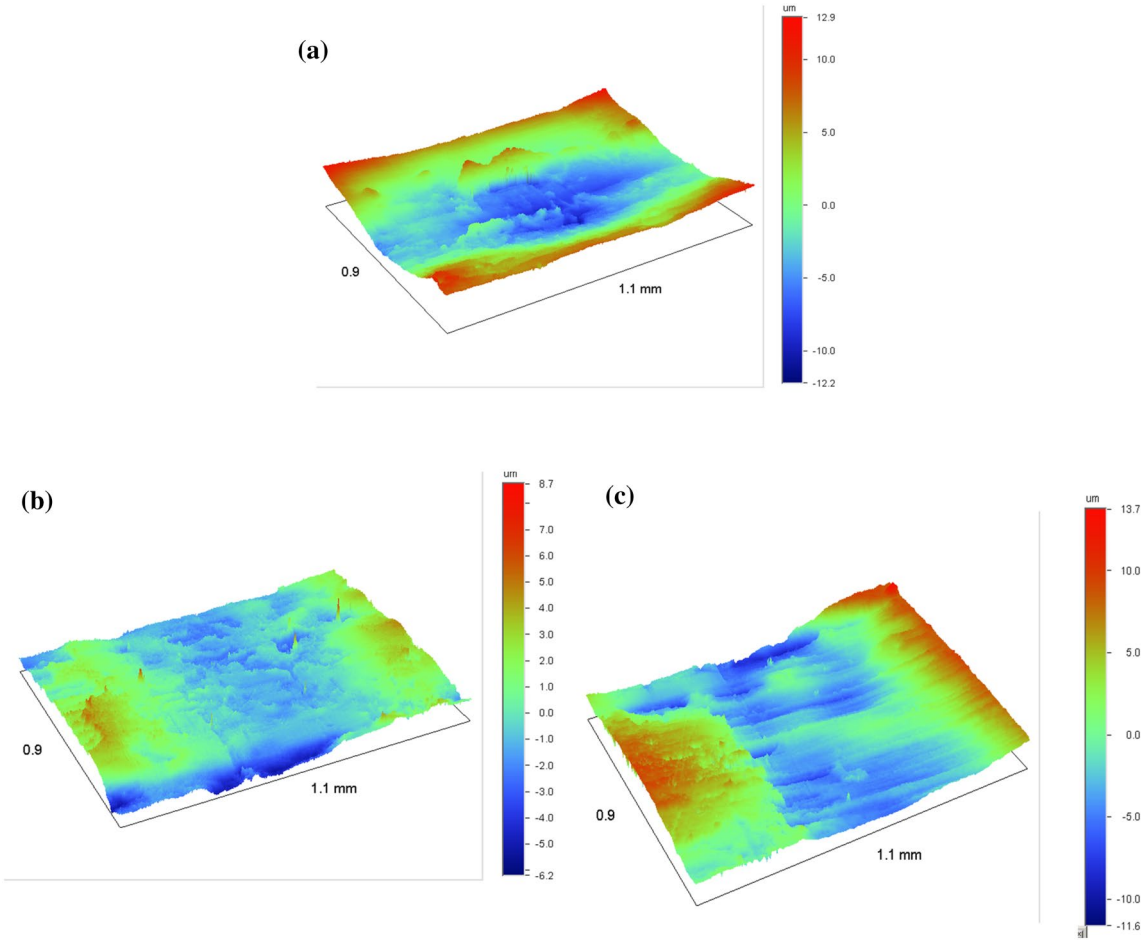

Fig. 7 Three-dimensional topographic relief observed on the wear track of the different biocomposites; **a** unfilled HDPE, **b** 5-wt% MS–HDPE, and **c** 10-wt% MS–HDPE after tribocorrosion tests in bovine serum solution

The use of MS fillers strongly influenced the wear of HDPE morphologies. In fact, the addition of 5 wt% of MS (Fig. 7b) presents a smoother topographic relief compared to unfilled HDPE.

However, with the addition of the 10 wt% of MS particles (Fig. 7c–f), deep grooves accompanied by material pull-out are observed in the wear track.

Figure 8 shows cross-sectional views of the wear profiles developed on the different wear traces of composites, 0, 5, and 10 wt% of MS–HDPE, after 15,000 sliding cycles in bovine serum solution. A deeper wear profile, 12.2 µm, is observed for 0 wt% of MS–HDPE, in which the material is displaced to the sides due to plastic flow, forming ridges (Fig. 8a). For 5 and 10 wt% of MS–HDPE, maximum wear depths of 6.2 µm and 11.6 µm were measured, respectively (Fig. 8b, c). The reduction is explained by the higher surface hardness of the composite material. In addition, with the addition of the MS particles, the wear trace has an irregular hemispherical shape (Fig. 8b, c). This reflects the removal of reinforcement particles during friction.

The SEM images after tribocorrosion tests in the presence of bovine serum solution of various biocomposite wear tracks are given in Fig. 9.

This figure shows that the wear tracks of unfilled HDPE and its biocomposites have different wear morphologies. The wear surface of unfilled HDPE (Fig. 9a, b) appears to be smoother than that observed in dry conditions as described in our previous study [23]. Indeed, Crockett et al. [40] showed that albumin from bovine serum adsorbs to the polymer in the form of a homogeneous layer. In addition, as reported in the literature [17, 41] a hydrophobic surface, such as HDPE, makes it easier to spread the albumin layer on its surface than on a hydrophilic surface [41]. Consequently, the smooth aspect observed on the wear track of unfilled HDPE is probably due to the formation of an albumin layer on the surface of the polymer. The examination of Fig. 9a shows that unfilled HDPE has been damaged by material removal, where several cavities are present in the wear track. As friction in bovine serum, a set of HDPE wear debris were generated. At higher magnification, plastic deformations and HDPE debris were observed in the wear track (Fig. 9b). These phenomena were also observed by Salem et al. [22].

With the addition of 5 wt% of MS (Fig. 9c), the surface of the wear track presents discontinuous, parallel, and shallow grooves in the sliding direction with moderate removal material. In addition, Fig. 9c shows the presence of a relatively large debris generated in the wear track with the presence of microcracks in the tribofilm. With 10 wt% of MS, scratches parallel to the sliding direction are observed in Fig. 9e. These scratches seem to be more pronounced than those observed with 5 wt% of MS.

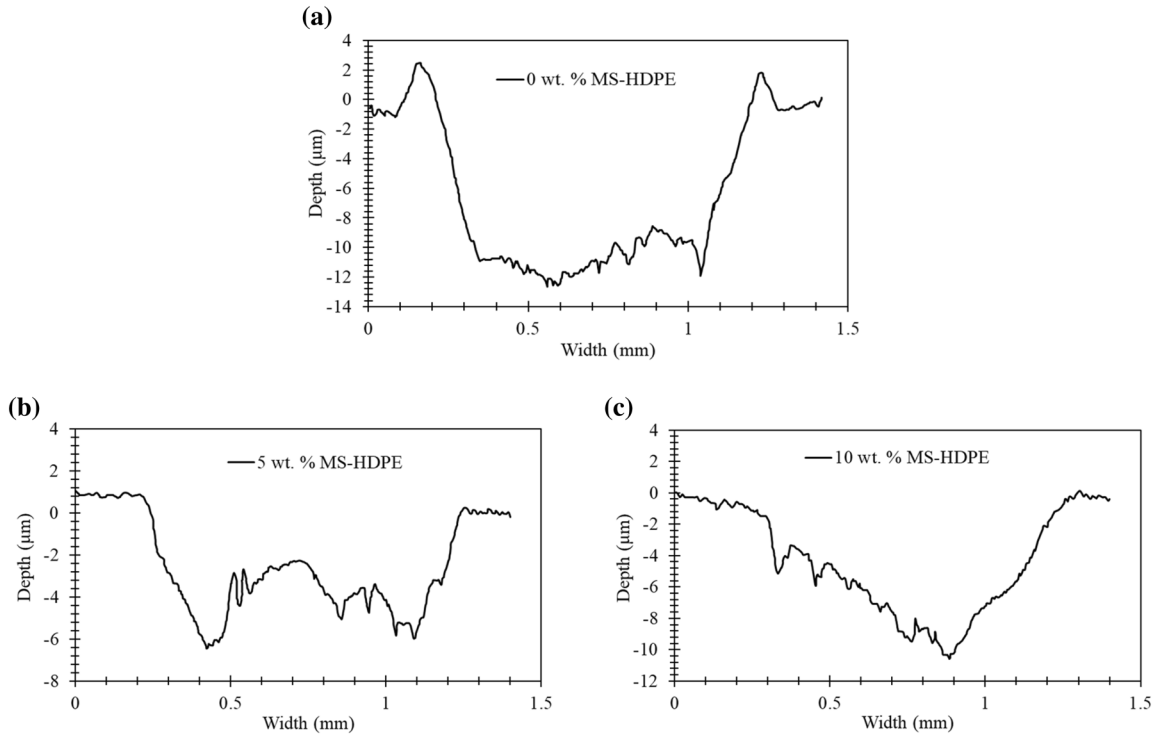

Fig. 8 Wear profiles of **a** 0-wt% MS–HDPE, **b** 5-wt% MS–HDPE, and **c** 10-wt% MS–HDPE after linear reciprocating wear tests under bovine serum solution

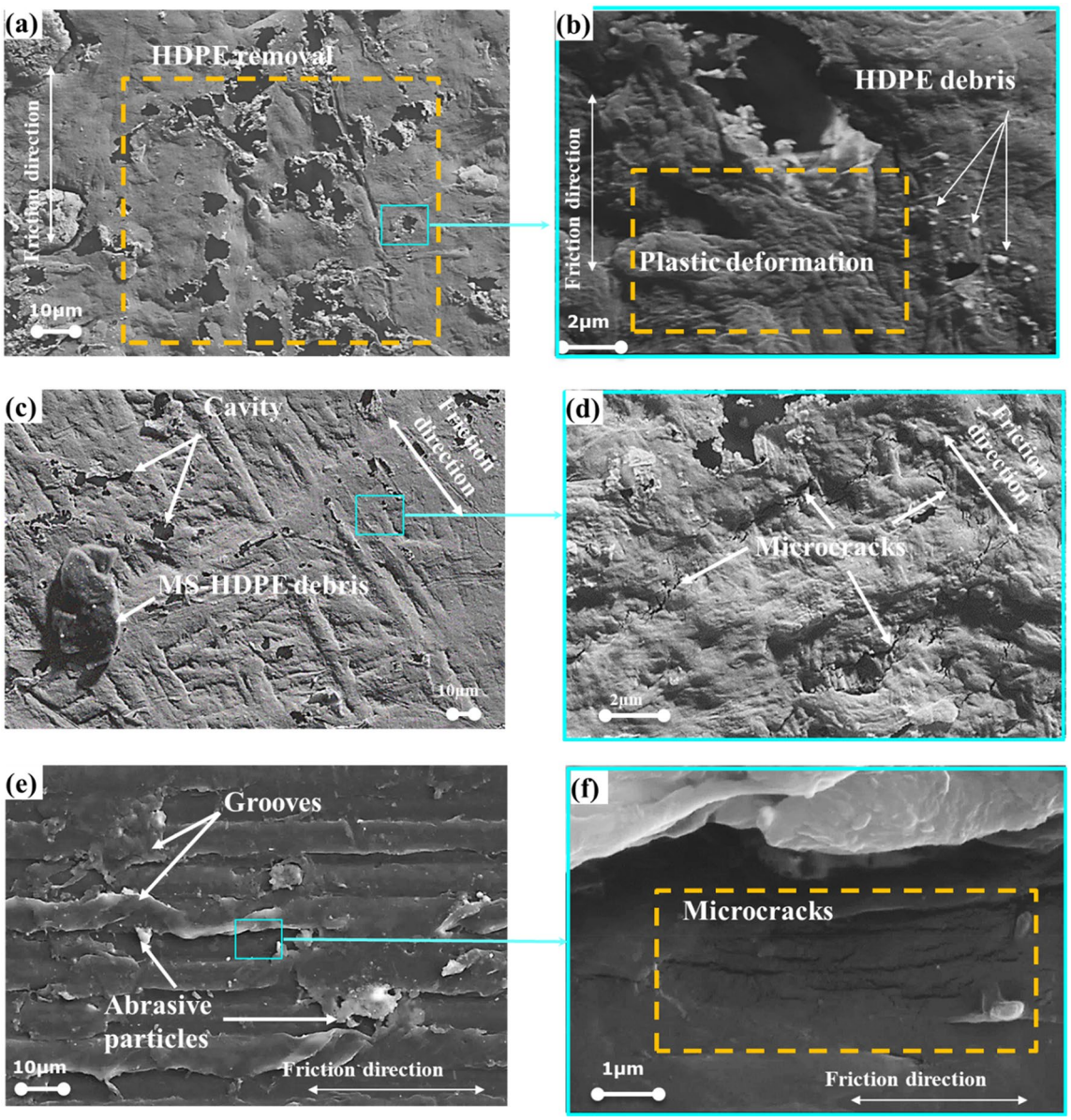

Fig. 9 Morphology of the wear track after tribocorrosion tests of **a**, **b** unfilled HDPE, **c**, **d** 5-wt% MS–HDPE, and **e**, **f** 10-wt% MS–HDPE in bovine serum solution

At higher magnification, parallel microcracks in the sliding direction are observed (Fig. 9f). These microcracks appear to be the cause of polymer fatigue [17]. SEM images confirm that 5-wt% MS–HDPE presents a better surface morphology compared to 10-wt% MS–HDPE. This result is probably related to the good distribution of a small amount of filler in the matrix. This result correlates with previous study of Li et al. [42].

3.5 Damage Modes and Wear Scenario

The adsorption of bovine serum proteins on the polymer and metal surfaces, certainly, has an effect on the wear mechanism. In the presence of bovine serum on the Ti6Al4V titanium alloy, the passive film comprises a protein-rich inner layer and an oxide outer layer. The proteins from the serum adhere to the titanium surface, forming a protective barrier

that prevents direct contact with the environment and contributes to biocompatibility. The outer oxide layer, primarily composed of titanium dioxide (TiO_2), functions as an additional physical barrier [31, 41].

In addition, several studies in the literature have shown that the hydrophobic surface of polyethylene promotes the adsorption of albumin [26, 43, 44]. Therefore, before sliding, an albumin layer is formed on the surface of the HDPE and its biocomposite (Fig. 10).

However, Lee et al. [45] have shown that protein adsorption increases with the crystallinity of the polymer. As the addition of MS to HDPE increases its crystallinity as demonstrated in our previous study [23], a thick tribofilm layer of albumin will be formed on the surface of the biocomposite before friction (Fig. 10a).

The MS–HDPE composite exhibits a specific mode of damage during sliding contact. In the first friction cycles, the albumin layer formed on the metal rubs against that formed on the biocomposite surface. By increasing the number of friction cycles, a peeling of the albumin layer will take place on both the metal and the composite (Fig. 10b). This detachment of the albumin layer can influence the wear and morphology of the materials in contact [38]. Several wear mechanisms have been identified, including grooving, plastic deformation, and passive film formation. Grooving is manifested by the presence of parallel grooves along the wear zone, resulting from the removal of material during abrasive wear. Plastic deformation occurs when material is displaced to the sides of the grooves due to plastic flow. In addition, a thin layer of titanium dioxide (TiO_2) forms on the surface of the Ti6Al4V titanium alloy. This layer can be seen in Fig. 10, where it is distinguished by the accumulation of worn materials interacting with the bovine serum solution. This wear corresponds to the tribo-oxidative wear mode.

Moreover, in the case of HDPE friction, it is well known that the HDPE debris transfers and adheres as films to the hard counter body [17]. Indeed, direct friction between the metal and the biocomposite can lead to the generation of MS–HDPE debris. Subsequently, other MS–HDPE debris coated by albumin acts as a third body in the tribological system, generating scratches and cavities on the biocomposite surface. This wear corresponds to the abrasive wear of the composite surface.

Toward the end of the friction process, the albumin that coats the composite debris reacts with the metal, resulting in the re-formation of a protective layer on the metal's surface.

4 Conclusion

The present study investigates the tribocorrosion behavior of MS–HDPE biocomposite against Ti6Al4V pin in the presence of bovine serum solution.

The following conclusions can be drawn from the obtained results:

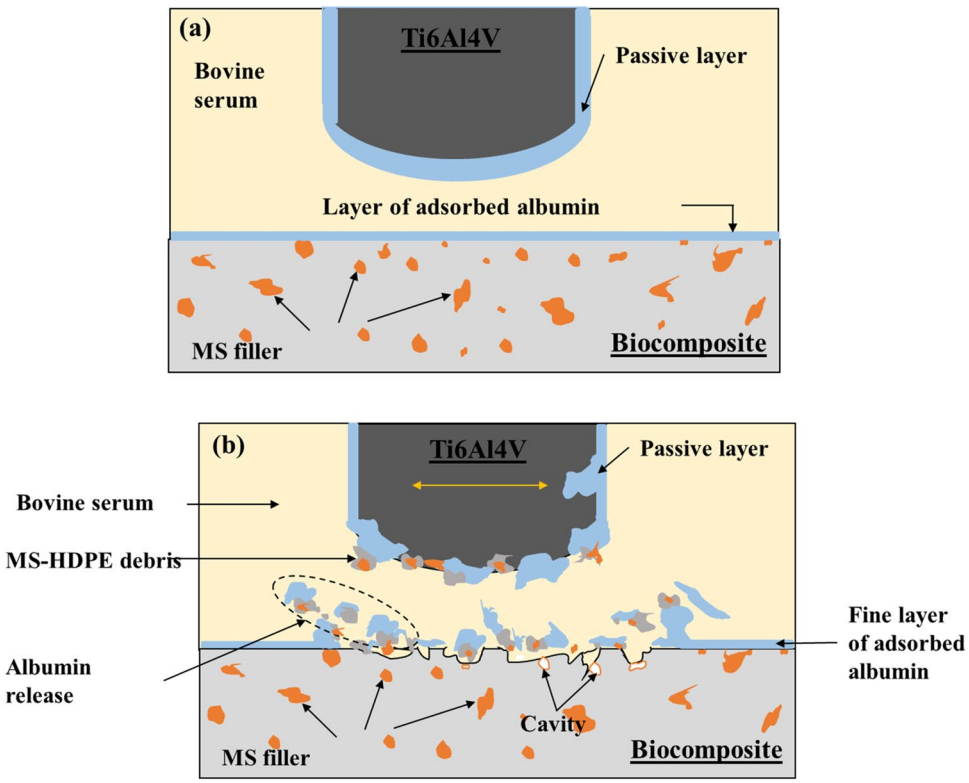

Fig. 10 Biocomposite wear scenario **a** before friction and **b** after the tribocorrosion test

(i) Prior to friction, the open-circuit potential (OCP) of the Ti6Al4V pin shifted toward positive potentials due to the formation of a protective passive film triggered by bovine serum. During friction, the presence of MS particles influenced the mechanism of passive film formation on the Ti6Al4V pin. Notably, when the biocomposite contained 15 wt% of MS, the passive film on the pin degraded. This phenomenon has been reported to the presence of more MS debris at the friction interface.

(ii) Under dry conditions, the inclusion of MS particles in the HDPE matrix significantly reduced the friction coefficient and specific wear rate. However, in the presence of bovine serum, the addition of MS particles led to an increased coefficient of friction, attributed to the formation of an albumin tribofilm on the biocomposite surface.

(iii) Compared to dry conditions, the biocomposites containing 5, 10, and 15 wt% of MS exhibited improved wear behavior in the presence of bovine serum solution. Specifically, the inclusion of 5 wt% of MS resulted in a 50% reduction in the specific wear rate in the bovine serum solution.

(iv) The wear morphology of the biocomposite surfaces differed in the presence of bovine serum solution. Various wear mechanisms, including grooving, plastic deformation, and passive film formation, were identified. Notably, the 5-wt% MS–HDPE biocomposite exhibited superior wear morphology when subjected to bovine serum.

Acknowledgements The authors would like to express their gratitude to the University of Monastir and the Ministry of Higher Education and Scientific Research—Tunisia for their support (LGM: LAB-MA-05). Special thanks are also extended to Mr. Didier Voillemin, the manager of C2T Implants, for his invaluable cooperation during the course of this study. The authors express their gratitude for the valuable support provided by Lyon University-France, including IMT Mines Saint-Étienne, Center CIS, and UMR INSERM 1059 SainBioSE, in conducting the tribocorrosion tests.

Author Contributions BS contributed to experimentation, methodology, and writing and original draft preparation. WB contributed to validation and reviewing of the manuscript. All authors reviewed the manuscript

Funding The author(s) received no financial support for the research, authorship, and/or publication of this article.

Data Availability The data that support the findings of this article are available in Journal of Bio- and Tribo-Corrosion website (Springer).

Declarations

Conflict of interest The authors declare that they have no known competing financial interests or personal relationships that could have appeared to influence the work reported in this paper.

Ethical Approval Applicable for both human and/or animal studies. Ethical Committees, Internal Review Boards, and guidelines followed must be named.

Informed Consent When applicable, additional headings with statements on consent to participate and consent to publish are also required. Not applicable.

References

1. Doctorale E, Monnet UJ (2019) Tribologie du Ti–6AI–4V et d' un revêtement DLC en fretting : applications au contact tige / col dans les prothèses de hanches modulaires Haohao Ding To cite this version : HAL Id : tel-02076289 Matériaux Tribology of Ti–6Al–4V and DLC coating in FRE.
2. Merola M, Affatato S (2019) Materials for hip prostheses: a review of wear and loading considerations. Materials (Basel). https://doi.org/10.3390/ma12030495
3. Yan Y (2013) Bio-tribocorrosion in biomaterials and medical implants. https://doi.org/10.1533/9780857098603
4. Basa S, Benea L (2014) Tribocorrosion—insight into material degradation in specific environments. http://10.11.10.50/xmlui/handle/123456789/5265
5. Siopack JS, Jergesen HE (2018) Total hip arthroplasty. https://doi.org/10.2788/31286
6. Xu Y, Qi H, Li G, Guo X, Wan Y, Zhang G (2018) Significance of an in situ generated boundary film on tribocorrosion behavior of polymer–metal sliding pair. J Colloid Interface Sci 518:263–276. https://doi.org/10.1016/j.jcis.2018.02.037
7. Yan Y (2006) Corrosion and tribo-corrosion behaviour of metallic orthopaedic implant materials. PhD, School of Mechanical Engineering, p 255
8. Pellier J, Geringer J, Forest B (2011) Fretting-corrosion between 316L SS and PMMA: influence of ionic strength, protein and electrochemical conditions on material wear. Application to orthopaedic implants. Wear 271:1563–1571. https://doi.org/10.1016/j.wear.2011.01.082
9. Boulila A, Jendoubi K, Zghal A, Khadhraoui M, Chabrand P (2010) Comportement mécanique des prothèses totales de hanche au pic de chargement. Mec Ind 11:25–36. https://doi.org/10.1051/meca/2010013
10. Azzi M, Szpunar JA (2007) Tribo-electrochemical technique for studying tribocorrosion behavior of biomaterials. Biomol Eng 24:443–446. https://doi.org/10.1016/j.bioeng.2007.07.015
11. Gras P (2014) Etude Physico-Chimique Et Structurale De Pyrophosphates De Calcium Hydrates: Application Aux Micro-Calcifications Associees a L'Arthrose, p 208
12. Medacta (n.d.) https://www.medacta.com/FR/hip-replacement
13. Grigoriadou I, Pavlidou E, Paraskevopoulos KM, Terzopoulou Z, Bikiaris DN (2018) Comparative study of the photochemical stability of HDPE/Ag composites. Polym Degrad Stab 153:23–36. https://doi.org/10.1016/j.polymdegradstab.2018.04.016
14. Gilbert JL, Mali SA (2012) Medical implant corrosion: electrochemistry at metallic biomaterial surfaces. In: Eliaz N (ed) Degradation of implant materials. Springer, pp 1–28. https://doi.org/10.1007/978-1-4614-3942-4_2
15. López-Ortega A, Arana JL, Bayón R (2018) Tribocorrosion of passive materials: a review on test procedures and standards. Int J Corros. https://doi.org/10.1155/2018/7345346
16. Salem A, Bensalah W, Mezlini S (2019) Tribological investigation of HDPE-cuttlebone and HDPE-red coral composites. J Bionic Eng 16:1068–1079. https://doi.org/10.1007/s42235-019-0119-z

17. Manoj Kumar R, Gupta P, Sharma SK, Mittal A, Shekhar M, Kumar V, Manoj Kumar BV, Roy P, Lahiri D (2017) Sustained drug release from surface modified UHMWPE for acetabular cup lining in total hip implant. Mater Sci Eng C 77:649–661. https://doi.org/10.1016/j.msec.2017.03.221
18. Chris-okafor PU, Okonkwo CC, Ohaeke MS (2018) Reinforcement of high density polyethylene with snail shell powder. Am J Polym Sci 8:17–21. https://doi.org/10.5923/j.ajps.20180801.03
19. Coringa R, de Sousa EM, Botelho JN, Diniz RS, de Sa JC, da Cruz MCFN, Paschoal MAB, Gonçalves LM (2018) Bone substitute made from a Brazilian oyster shell functions as a fast stimulator for bone-forming cells in an animal model. PLoS ONE 13:1–13. https://doi.org/10.1371/journal.pone.0198697
20. Buciumeanu M, Araujo A, Carvalho O, Miranda G, Souza JCM, Silva FS, Henriques B (2016) Study of the tribocorrosion behaviour of Ti6Al4V–HA biocomposites. Tribol Int 107:77–84. https://doi.org/10.1016/j.triboint.2016.11.029
21. Zai W, Wong MH, Man HC (2019) Improving the wear and corrosion resistance of CoCrMo-UHMWPE articulating surfaces in the presence of an electrolyte. Appl Surf Sci 464:404–411. https://doi.org/10.1016/j.apsusc.2018.09.027
22. Salem A, Guezmil M, Bensalah W, Mezlini S (2019) Tribological behavior of molybdenum disulphide particles-high density polyethylene composite. Mater Res Express 6:075402
23. Sidia B, Bensalah W (2020) Tribological properties of High Density Polyethylene based composite: the effect of mollusc shell particles under dry condition. J Compos Mater. https://doi.org/10.1177/0021998320965655
24. García-León RA, Martínez-Trinidad J, Campos-Silva I, Figueroa-López U, Guevara-Morales A (2021) Development of tribological maps on borided AISI 316L stainless steel under ball-on-flat wet sliding conditions. Tribol Int. https://doi.org/10.1016/j.triboint.2021.107161
25. Huang J, Qu S, Wang J, Yang D, Duan K, Weng J (2013) Reciprocating sliding wear behavior of alendronate sodium-loaded UHMWPE under different tribological conditions. Mater Sci Eng C 33:3001–3009. https://doi.org/10.1016/j.msec.2013.03.030
26. Widmer MR, Heuberger M, Vörös J, Spencer ND (2001) Influence of polymer surface chemistry on frictional properties under protein-lubrication conditions: implications for hip-implant design. Tribol Lett 10:111–116. https://doi.org/10.1023/A:1009074228662
27. López-Ortega A, Arana JL, Bayón R (2020) On the comparison of the tribocorrosion behavior of passive and non-passivating materials and assessment of the influence of agitation. Wear. https://doi.org/10.1016/j.wear.2020.203388
28. Contu F, Elsener B, Bhni H (2002) Characterization of implant materials in fetal bovine serum and sodium sulfate by electrochemical impedance spectroscopy. I. Mechanically polished samples. J Biomed Mater Res 62:412–421. https://doi.org/10.1002/jbm.10329
29. Cheng X, Roscoe GS (2005) Corrosion behavior of titanium in the presence of calcium phosphate and serum proteins. Biomaterials 26:7350–7356. https://doi.org/10.1016/j.biomaterials.2005.05.047
30. Royhman D, Patel M, Runa MJ, Wimmer MA, Jacobs JJ, Hallab NJ, Mathew MT (2016) Fretting-corrosion behavior in hip implant modular junctions: the influence of friction energy and pH variation. J Mech Behav Biomed Mater 62:570–587. https://doi.org/10.1016/j.jmbbm.2016.05.024
31. Masdek NRN, Rozali AA, Murad MC, Salleh Z (2018) Effect of protein concentration on corrosion of Ti–6Al–4V and 316L SS alloys. ISIJ Int 58:1519–1523. https://doi.org/10.2355/isijinternational.ISIJINT-2018-183
32. Gibson LJ, Ashby MF, Harly BA (2010) Cellular materials in nature and medicine. Cambridge University Press, Cambridge
33. More NS, Diomidis N, Paul SN, Roy M, Mischler S (2011) Tribocorrosion behavior of β titanium alloys in physiological solutions containing synovial components. Mater Sci Eng C 31:400–408. https://doi.org/10.1016/j.msec.2010.10.021
34. Souza JCM, Barbosa SL, Ariza E, Celis JP, Rocha LA (2012) Simultaneous degradation by corrosion and wear of titanium in artificial saliva containing fluorides. Wear 292–293:82–88. https://doi.org/10.1016/j.wear.2012.05.030
35. Yan Y, Wang L, Neville A, Qiao L (2013) Tribofilm on hip implants. Orthop Trauma 27:93–100. https://doi.org/10.1016/j.mporth.2013.02.006
36. Mary N, Geringer J, Corse LM (2013) Tribocorrosion. https://doi.org/10.13140/2.1.4488.0968
37. Saikko V (2003) Effect of lubricant protein concentration on the wear of ultra-high molecular weight polyethylene sliding against a CoCr counterface. J Tribol 125:638–642. https://doi.org/10.1115/1.1537751
38. Dwivedi Y, Laurent MP, Sarvepalli S, Schmid TM, Wimmer MA (2017) Albumin protein cleavage affects the wear and friction of ultra-high molecular weight polyethylene. Lubricants. https://doi.org/10.3390/lubricants5030033
39. Jagatheeshwaran MS, Elayaperumal A, Arulvel S (2016) The role of calcinated sea shell particles on friction-wear behavior of electroless NiP coating: fabrication and characterization. Surf Coat Technol 304:492–501. https://doi.org/10.1016/j.surfcoat.2016.07.053
40. Crockett R, Roba M, Naka M, Gasser B, Delfosse D, Frauchiger V, Spencer ND (2009) Friction, lubrication, and polymer transfer between UHMWPE and CoCrMo hip-implant materials: a fluorescence microscopy study. J Biomed Mater Res A 89:1011–1018. https://doi.org/10.1002/jbm.a.32036
41. Rabe M, Verdes D, Seeger S (2011) Understanding protein adsorption phenomena at solid surfaces. Adv Colloid Interface Sci 162:87–106. https://doi.org/10.1016/j.cis.2010.12.007
42. Li HY, Tan YQ, Zhang L, Zhang YX, Song YH, Ye Y, Xia MS (2012) Bio-filler from waste shellfish shell: preparation, characterization, and its effect on the mechanical properties on polypropylene composites. J Hazard Mater. https://doi.org/10.1016/j.jhazmat.2012.03.028
43. Serro AP, Degiampietro K, Colaço R, Saramago B (2010) Adsorption of albumin and sodium hyaluronate on UHMWPE: a QCM-D and AFM study. Colloids Surf B 78:1–7. https://doi.org/10.1016/j.colsurfb.2010.01.022
44. Karuppiah KSK, Sundararajan S, Xu ZH, Li X (2006) The effect of protein adsorption on the friction behavior of ultra-high molecular weight polyethylene. Tribol Lett 22:181–188. https://doi.org/10.1007/s11249-006-9078-8
45. Lee WH, Zavgorodniy AV, Loo CY, Rohanizadeh R (2012) Synthesis and characterization of hydroxyapatite with different crystallinity: effects on protein adsorption and release. J Biomed Mater Res A 100:1539–1549. https://doi.org/10.1002/jbm.a.34093

Publisher's Note Springer Nature remains neutral with regard to jurisdictional claims in published maps and institutional affiliations.

Springer Nature or its licensor (e.g. a society or other partner) holds exclusive rights to this article under a publishing agreement with the author(s) or other rightsholder(s); author self-archiving of the accepted manuscript version of this article is solely governed by the terms of such publishing agreement and applicable law.